Comparison of the standards for absorbed dose to water of the METAS, Switzerland and the BIPM in accelerator photon beams

C. Kessler [1], D.T. Burns [1], P. Roger[1], C. Kottler [2], S. Vörös [2], P. Peier [2]

[1] Bureau International des Poids et Mesures, F-92310 Sèvres Cedex
[2] Federal Institute of Metrology (METAS), Bern, Switzerland

Abstract

A key comparison has been carried out of the absorbed dose to water standards of the Federal Institute of Metrology (METAS), Switzerland, and the BIPM in accelerator photon beams. The results show the standards to be in agreement within the standard uncertainty of the comparison of 6.6 parts in 10^3. The results are analysed and presented in terms of degrees of equivalence, suitable for entry in the BIPM key comparison database.

1. Introduction

An indirect comparison has been made between the absorbed dose to water standards of the Federal Institute of Metrology (METAS), Switzerland, and the Bureau International des Poids et Mesures (BIPM) in the accelerator photon beam range from 6 MV to 18 MV. The comparison took place using BIPM instrumentation at the DOSEO accelerator facility in Saclay (France) in June 2018. The comparison was undertaken using two transfer ionization chambers type NE 2571 and NE 2611 of the METAS. The results of the comparison are given in terms of the mean ratio of the calibration coefficients of these transfer instruments determined at the two laboratories for three radiation qualities. The final results were supplied by the METAS in June 2018.

2. Details of the standards

BIPM primary standard

The BIPM primary standard is a graphite calorimeter described by Picard *et al.* (2009). The calorimeter consists of a graphite core placed in a cylindrical graphite jacket; the main characteristics are listed in Table 1. The core is equipped with three thermistor pairs connected to three independent d.c. bridges. This core and jacket are placed in an evacuated cubic PMMA vacuum phantom with side length 300 mm. A graphite build-up plate is used to position the calorimeter centre at the reference depth of 10 g cm^{-2}. Two nominally-identical

parallel-plate ionization chamber standards with graphite walls and collector, similar in design to the existing BIPM standards for air kerma and absorbed dose to water, were fabricated to serve in the determination of the absorbed dose to water from the measured absorbed dose to the graphite core. The first chamber is housed in a graphite jacket, nominally identical to the calorimeter jacket, and is positioned in the same PMMA vacuum phantom but at ambient air pressure, replacing the calorimeter core and its jacket. The second chamber is housed in a waterproof polyethylene sleeve and mounted at a depth of 10 g cm^{-2} in a PMMA water phantom with the same outer dimensions and PMMA window thickness (4 mm) as the vacuum phantom.

Table 1. Characteristics of the BIPM standard

BIPM standard		Dimensions
Calorimeter core	Diameter / mm	45.0
	Thickness / mm	6.7
Calorimeter jacket	Diameter / mm	60.0
	Thickness / mm	32.0
Standard chamber	Diameter / mm	45.0
	Thickness / mm	11.0
Air cavity	Volume / cm^3	6.8
Wall	Thickness / mm	2.85
	Material	Graphite
	Density / g cm^{-3}	1.85
Voltage applied to outer electrode / V	Positive polarity	80

METAS Primary standard

The METAS primary standard for absorbed dose to water is a water calorimeter, described by Medin *et al* (1999). The detector is a glass vessel filled with ultra-pure water saturated with various gases, in which 2 NTC probes measure the temperature increase due to the absorbed radiation energy, positioned in a thermally isolated cubic water phantom with 30 cm length sides.

3. Determination of the absorbed dose to water

3.1 Absorbed dose to water at the BIPM

At the BIPM the absorbed dose to water rate is determined from calorimetric and ionometric measurements combined with Monte Carlo calculations. The method is described in Burns (2018) and in a number of previous comparison reports, for example Picard *et al* (2016). The absorbed dose to water at the reference depth, $D_{\mathrm{w,BIPM}}$, is evaluated as:

$$D_{\mathrm{w,BIPM}} = D_{\mathrm{c}} \frac{Q_{\mathrm{w}}}{Q_{\mathrm{c}}} \left(\frac{D_{\mathrm{w}}}{D_{\mathrm{c}}}\right)^{\mathrm{MC}} \left(\frac{D_{\mathrm{cav,c}}}{D_{\mathrm{cav,w}}}\right)^{\mathrm{MC}} k_{\mathrm{rn}} \qquad (1)$$

where

D_{c} measured absorbed dose to the graphite core;

Q_{c} ionization charge measured by the standard chamber positioned in

the graphite jacket, replacing the core;

Q_w ionization charge measured by the standard chamber positioned in water;

$(D_w/D_c)^{MC}$ calculated ratio of absorbed dose to water and to the graphite core using Monte Carlo simulations;

$\left(D_{cav,c}/D_{cav,w}\right)^{MC}$ calculated ratio of cavity doses in graphite and in water using Monte Carlo simulations;

k_{rn} measured correction for radial non-uniformity in water.

The ionization charges Q_w and Q_c are normalized to 293.15 K and 101.325 kPa and corrected for ion recombination, as explained at the end of this section. In practice, two nominally-identical standard chambers are used; the air cavity volume for each is known and a correction k_{vol} is made for the small difference in volume with a relative standard uncertainty of 3 parts in 10^4.

Equation 1 can also be expressed as

$$D_{w,BIPM} = Q_w \frac{D_c}{Q_c} C_{w,c} k_{rn} = Q_w N_{D_c} C_{w,c} k_{rn} \quad (2)$$

where

$C_{w,c}$ represents the total Monte Carlo conversion factor;

N_{D_c} is the measured calibration coefficient for the standard chamber in graphite.

- *Monte Carlo conversion factor $C_{w,c}$*

During the period 2009-2015, twenty calculations of the conversion factor $C_{w,c}$ were carried out using the sets of phase-space files provided by the National Metrology Institutes (NMIs) that participated in the BIPM.RI(I)-K6 key comparison. Figure 1 shows the conversion factors plotted as a function of the calculated $TPR_{20,10}$; a quadratic fit to these data, weighted with the statistical uncertainty of each point, shows the deviations to be consistent with the typical statistical standard uncertainty of 5 parts in 10^4. For the present comparison, the dose conversion factors presented in Table 2 are obtained using the quadratic fit and the $TPR_{20,10}$ values measured at the DOSEO facility. A type A uncertainty of 5 parts in 10^4 arising from the fitting procedure is included in Table 10, as well as the type B uncertainty for $C_{w,c}$ of 2.5 parts in 10^3 derived from Burns (2018).

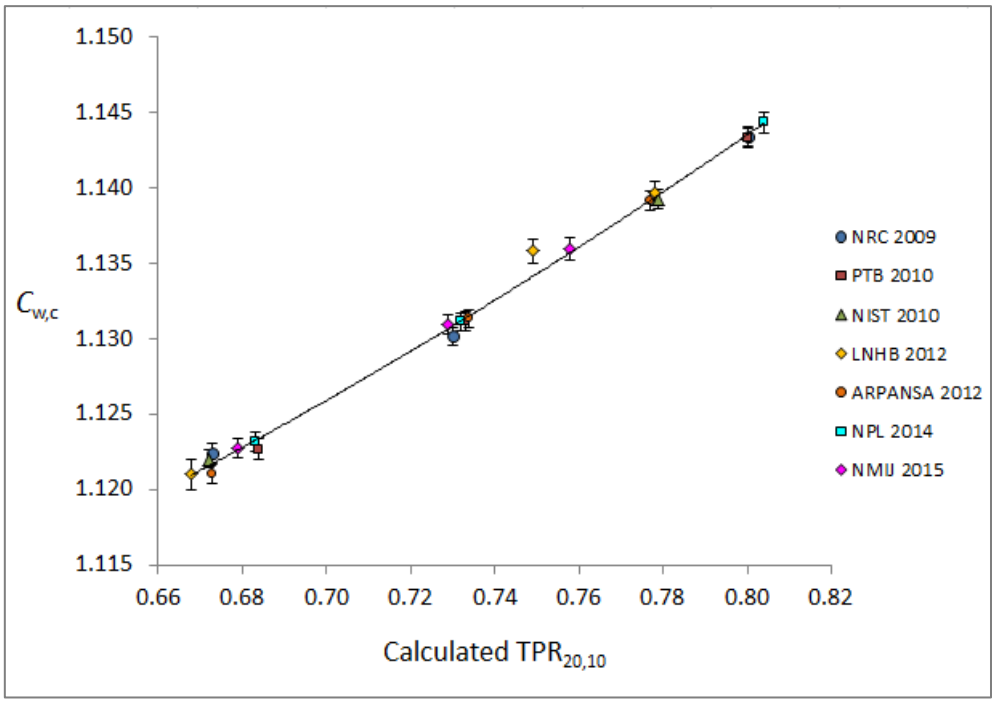

Figure 1. The dose conversion factor $C_{w,c}$ for the BIPM standard, calculated using the phase-space files supplied by participating NMIs. The line is a weighted quadratic fit to the data; the deviations about this line are consistent with the typical statistical standard uncertainty of 5 parts in 10^4.

- *Calibration coefficient N_{D_c}*

During each comparison, the calibration coefficient N_{D_c} for the standard chamber in graphite has been measured and plotted as a function of the measured $TPR_{20,10}$. Figure 2 shows the normalized N_{D_c} determinations and a quadratic fit to the data; the plot also shows the coefficients determined at the DOSEO facility, which are included in the fit.

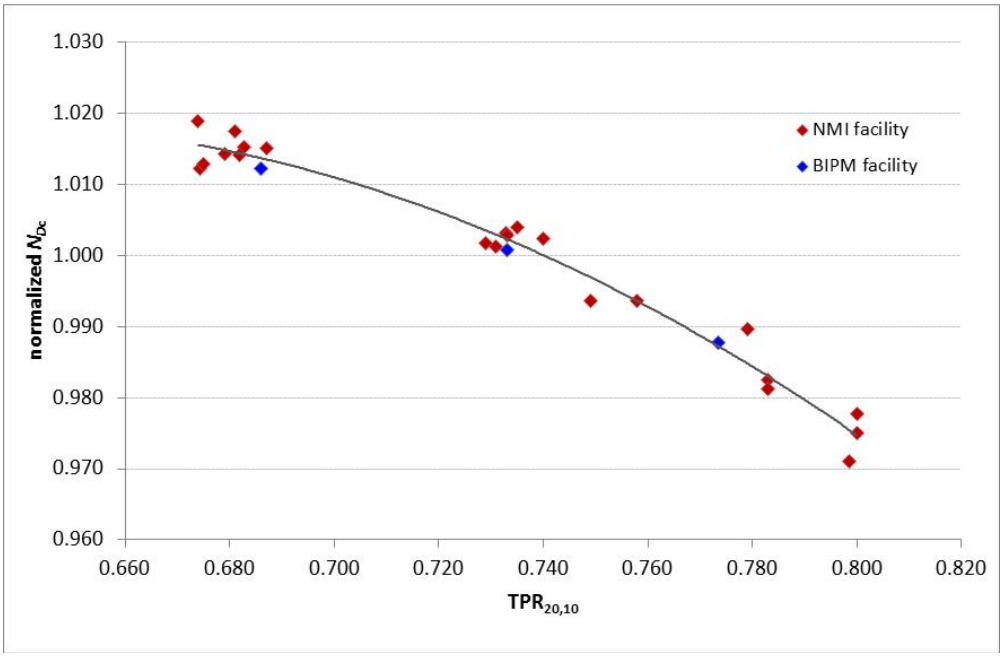

Figure 2. The calibration coefficients N_{Dc}, normalized to the mean, as a function of the measured $TPR_{20,10}$. The solid line is a quadratic fit to the combined data set.

For the present comparison, the calibration coefficients N_{D_c} for the standard chamber in graphite for the BIPM $TPR_{20,10}$ values are taken to be those derived from the quadratic fit and are presented in Table 2. The uncertainty arising from the fitting procedure is taken as the r.m.s. deviation of the measured values from the fitted curve (2.3 parts in 10^3) and is included in Table 10. By its nature, this includes the statistical uncertainties associated with the BIPM calorimeter and well as those arising from differences in spectra at the NMI accelerators.

Table 2. BIPM conversion factors and calibration coefficients

Radiation quality	6 MV	10 MV	18 MV
$TPR_{20,10}$	0.686	0.733	0.774
$C_{w,c}$ (fit)	1.1229	1.1306	1.1377
N_{D_c} (fit)	4.011	3.966	3.906

As mentioned above, the ionization charges Q_w and Q_c are normalized to 293.15 K and 101.325 kPa; no correction for humidity is applied. The temperature is measured using a calibrated thermistor, placed inside the water-proof envelope and inside the graphite jacket for measurements in water and graphite, respectively.

The ionization charges Q_w and Q_c are corrected for ion recombination. The correction factor k_s for losses due to ion recombination for the standard chambers in graphite and water were determined using the method of Niatel as described by Boutillon (1998).

The recombination correction k_s can be expressed as:

$$k_s = 1 + k_{\text{init}} + k_{\text{vol}} Q_p \qquad (3)$$

where Q_p is the charge per pulse expressed in pC. Table 3 gives the values for k_{init} and k_{vol}. For a typical charge per pulse of up to 100 pC, k_s is of the order of 1 part in 10^2 and the standard uncertainty for k_s is estimated to be 5 parts in 10^4, as shown in Table 10.

Table 3. Ion recombination for the BIPM standard chambers

BIPM standard	Standard in water [a]	Standard in graphite [a]
initial recombination and diffusion, k_{init}	16.4×10^{-4}	18.8×10^{-4}
volume recombination coefficient, k_{vol} / pC^{-1}	1.43×10^{-4}	1.13×10^{-4}

[a] The standards in water and graphite are identified as CALO5 and CALO6c, respectively

The factors that correct for the non-uniformity of the beams were calculated from the measured beam profiles in water. For graphite, it is assumed that the correction cancels as the standard chamber in graphite has the same dimensions as the calorimeter core. The correction factors are listed in Table 4. A relative standard uncertainty of 1 part in 10^3 is introduced for this effect in Table 10.

Table 4. Radial non-uniformity correction in water

Radiation quality	6 MV	10 MV	18 MV
radial non-uniformity k_{rn}	0.9995	0.9928	1.0000

3.2 Absorbed dose to water at the METAS

At the METAS, the absorbed dose to water is determined using the equation

$$D_{\mathrm{w,METAS}} = C_p \Delta T \prod k_i \qquad (4)$$

where

C_p is the specific heat capacity at constant pressure;
ΔT is the measured temperature increase;
$\Pi\, k_i$ is the product of the correction factors to be applied to the standard.

The correction factors, k_i, applied in (4) are the following:

k_p is the effect of the perturbation of the radiation field due to the presence of the glass vessel and NTC probes; it was measured for each different vessel using a diode located at the reference depth;

k_c corrects for conductive heat flow due to the presence of glass, which has a different heat capacity from that of water, and to the presence of temperature gradients due to non-uniformities in the absorbed dose distribution; it was calculated using finite elements method software;

k_HD is the heat defect due to endothermic or exothermic chemical reactions in the water, which has been calculated using various models to be zero in pure water saturated with H_2, N_2 or Ar (Klassen and Ross 1991; Klassen and Ross 1997);

k_rho is the effect of the different water densities in calorimetric measurements at 4°C and in secondary standard measurements at 20 °C (in practice, the depth of measurement is determined in the units g cm^{-2} at both temperatures and hence no k_rho correction is needed);

k_v corrects for convective heat flow due to the temperature gradients in the water (convection does not take place when measuring at 4 °C, the temperature of maximum water density, hence k_v is unity);

k_t is the effect of transient behaviour of the thermistor just after the end of irradiation, which might affect the post-irradiation drift curve (in practice, data during the first 20 s after irradiation are discarded from the fit to avoid this effect).

The values for the specific heat capacity and the correction factors and their uncertainties are presented in Table 5. As noted above, the measurement conditions are chosen in such a way that the remaining factors are taken to be strictly unity, or 1.0000 with the corresponding uncertainty.

Table 5. METAS standard

METAS standard	value	u_c
Specific heat capacity C_p / J kg^{-1} K^{-1}	4204.84	2
Field perturbation k_p	1.0000	0.0003
Conductive heat flow k_c	0.9980	0.0015
Heat defect k_{HD}	1.0000	0.0030
Density k_{rho}	1.0000	–[a]
Convection k_v	1.0000	–
Transient thermistor response k_t	1.0000	< 0.0001

[a] included in depth in water (Table 12)

4. BIPM irradiation facility

4.1 The BIPM irradiation facility and reference beam qualities

The comparison was carried out in the DOSEO accelerator facility in Saclay (France), which houses an Elekta *Versa* linear clinical accelerator. This accelerator provides three high-energy photon beams at 6 MV, 10 MV and 18 MV. The radiation qualities are characterized in terms of the tissue-phantom ratio $TPR_{20,10}$, the measured values are given in Table 2. All measurements were made with the gantry fixed for horizontal irradiation, with a source-detector distance of 1 m and at the reference depth of 10 g cm^{-2}.

The irradiation area is temperature controlled at 20 °C. Calibrated thermistors measure the temperature of the ambient air and water. Air pressure is measured by means of a calibrated barometer positioned at the height of the beam axis. The relative humidity is controlled within the range from 40 % to 50 %.The beam output is monitored during irradiation using a commercial parallel-plate transmission chamber fixed to a shadow tray; the day-to-day stability of the transmission chamber is determined by comparing its response to a thimble chamber type NE 2571. This monitoring system is described in previous comparison reports, for example Picard *et al* (2016).

5. Comparison procedure

The comparison of the METAS and BIPM standards was carried out indirectly using the calibration coefficients $N_{D_w,\mathrm{lab}}$ for two transfer chambers given by

$$N_{D_\mathrm{w},\mathrm{lab}} = \dot{D}_{\mathrm{w,lab}} \big/ I_{\mathrm{lab}} \,, \qquad (5)$$

where $\dot{D}_{\mathrm{w,lab}}$ is the water absorbed dose rate at the laboratory, METAS or the BIPM, and I_{lab} is the corresponding ionization current for a transfer chamber measured at the laboratory.

The ionization chambers NE 2571, serial number 3168 and NE 2611, serial number 147, belonging to the METAS, were the transfer chambers used for this comparison. Their main characteristics are listed in Table 6.

Table 6. Characteristics of the transfer chambers NE 2571 and NE 2611

Transfer chambers - Nominal values		NE 2571	NE 2611
Dimensions of sensitive volume	radius / mm length / mm	3.2 24.1	3.7 9.2
Volume	air cavity / cm^3	0.7	0.3
Wall	material density / g cm^{-3}	graphite 1.7	graphite 1.7
Applied voltage	negative polarity to outer electrode / V	250	250

The essential details for the determination of the calibration coefficients N_{D_w} for the transfer chambers are described below.

Positioning

At each laboratory, the chambers were positioned with the stem perpendicular to the beam direction and with the appropriate marking on the stem and waterproof sleeve facing the source.

Applied voltage and polarity

A collecting voltage of 250 V (negative polarity) was applied to the outer electrode of the chambers at least 30 min before any measurements were made. No corrections were applied at either laboratory for polarity.

Ion recombination

Ion recombination was measured at the BIPM for each chamber using the method of Niatel (Boutillon 1998). The results are presented in Table 7. The correction factors were also determined using the two-voltage technique, as described in the IAEA protocol TRS 398 (IAEA 2000). The results are included in the table.

At the METAS, the correction for ion recombination was determined using the method of Niatel (Boutillon 1998). Using the coefficients determined at the METAS, the ion recombination correction was evaluated for the BIPM beams. The results are also included in the table.

The METAS results for ion recombination are in agreement with the BIPM (Niatel) values within the uncertainties stated in Tables 11 and 13.

Radial non-uniformity correction

The correction at the BIPM for the radial non-uniformity of the beam over the section of the transfer chambers is estimated to be 0.9980 and 0.9990 for the NE 2571 and NE 2611, respectively, for the quality 10 MV, and unity for the other two qualities, with an uncertainty of 5×10^{-4}. At the METAS, the following corrections are applied for the NE 2571 and the NE 2611, respectively: 0.9997 and 0.9987 for 6 MV, 0.9997 and 0.9990 for 10 MV and 0.9998 and 0.9995 for 18 MV. The estimated uncertainty is 1×10^{-3}.

Charge measurements

The charge Q was measured at the BIPM using a Keithley electrometer, model K6517B and a set of calibrated external capacitors. The chambers were pre-irradiated for at least 10 min (≈ 20 Gy) at the BIPM, and for at least 10 min (≈ 15 Gy) at the METAS before any measurements were made.

Table 7. Ion recombination for the NE 2571 and NE 2611 at the BIPM facility

Chamber	k_{init}	k_{vol} / pC^{-1}	$k_{s,transfer}$ 6 MV	10 MV	18 MV
NE 2571	17.2×10^{-4}	7.4×10^{-4}	1.0048	1.0071	1.0089
	TRS 398		1.0059	1.0074	1.0100
	METAS determination		1.0039	1.0063	1.0081
NE 2611	17.0×10^{-4}	1.5×10^{-4}	1.0045	1.0066	1.0081
	TRS 398		1.0056	1.0068	1.0077
	METAS determination		1.0041	1.0061	1.0077

Ambient conditions

At the BIPM, the water temperature is measured for each current measurement and it was stable to better than 0.1 °C. At the METAS, the water temperature was also measured for each current measurement and it was stable to better than 0.1 °C.

The ionization current is normalized to 293.15 K and 101.325 kPa at both laboratories. Relative humidity is in the range from 40 % to 50 % at the BIPM and from 45 % to 55 % at the METAS. Consequently, no correction for humidity is applied to the ionization current measured.

PMMA phantom window and sleeve

Both laboratories use a horizontal radiation beam and the thickness of the PMMA front window of the water phantom (4 mm at the BIPM and 2.58 mm at the METAS) is included as a water-equivalent thickness in g cm^{-2} when positioning the chamber.

Waterproof sleeves of 1 mm thick PMMA were supplied by the METAS for the transfer chambers. The same sleeves were used at both laboratories and, consequently, no correction for the influence of each sleeve was necessary at either laboratory.

6. Results of the comparison

Each transfer chamber was set-up and measured in the BIPM beams on two separate occasions. The results were reproducible to better than 1×10^{-3}. At the METAS, the chambers were calibrated by direct comparison with the calorimeter at 8 beam qualities with $TPR_{20,10}$ values from 0.639 to 0.802 (corresponding to an accelerating voltage from 4 MV to 21 MV). Subsequently, the following analytical function was fitted to the measured values of the calibration coefficients to obtain the parameters a, b and c:

$$N_{D_{w,TPR_{20,10}}} = a - \exp\left(b \cdot \exp\left(c \cdot TPR_{20,10}\right)\right) \quad (6)$$

This formula allows for the interpolation of the calibration coefficient at any value of the $TPR_{20,10}$. The values of the calibration coefficients for the transfer chambers, as stated in Table 8, were interpolated in this way for the comparison qualities given in Table 2.

No calibration against the calorimeter was performed in the high-energy photon beams after the measurements at the BIPM. Instead, to check the stability of the chambers, they were calibrated before and after the BIPM measurements in the ^{60}Co beam at the METAS. These results are assumed to apply to the high-energy beams and give rise to the relative standard uncertainty of 2 parts in 10^4 to represent the transfer chamber stability.

The result of the comparison, R_{D_w} , is expressed in the form

$$R_{D_w} = N_{D_w,\mathrm{METAS}} \big/ N_{D_w,\mathrm{BIPM}} \,, \qquad (7)$$

The results for each chamber are presented in Table 8.

Table 8. Calibration coefficients for the transfer chambers

Radiation quality	6 MV	10 MV	18 MV
NE 2571 -3168			
$N_{D_w,\mathrm{METAS}}$ / Gy μC^{-1}	44.79	44.42	43.94
$N_{D_w,\mathrm{BIPM}}$ / Gy μC^{-1}	44.88	44.56	43.98
NE 2611 -147			
$N_{D_w,\mathrm{METAS}}$ / Gy μC^{-1}	102.28	101.43	100.31
$N_{D_w,\mathrm{BIPM}}$ / Gy μC^{-1}	102.43	101.76	100.45

The final results $R_{D\mathrm{w,METAS}}$ in Table 9 are evaluated as the mean for the two transfer chambers. For each quality, the corresponding uncertainty s_{tr} is the standard uncertainty of this mean, derived from the difference in the two results. The mean value of s_{tr} for the three qualities, $s_{\mathrm{tr,comp}}$ = 0.0003, is a global representation of the comparison uncertainty arising from the transfer chambers and is included in Table 14.

Table 9. Comparison results

Radiation quality	6 MV	10 MV	18 MV
$N_{D_w,\mathrm{METAS}} \big/ N_{D_w,\mathrm{BIPM}}$ using NE 2571	0.9980	0.9969	0.9991
$N_{D_w,\mathrm{METAS}} \big/ N_{D_w,\mathrm{BIPM}}$ using NE 2611	0.9985	0.9968	0.9986
s_{tr}	0.0003	0.0001	0.0002
$R_{D\mathrm{w,METAS}}$	0.9983	0.9968	0.9988

The results shown in Table 9 demonstrate the agreement between the two standards for absorbed dose to water at the level of 2 or 3 parts in 10^3 which is within the relative standard uncertainty of the comparison of 6.6 parts in 10^3 evaluated below.

Uncertainties

The uncertainties associated with the BIPM primary standard are listed in Table 10 and those for the transfer chamber calibrations in Table 11.

Table 10. Uncertainties associated with the BIPM standard

Relative standard uncertainty [(1)]	$u_{i\mathrm{A}}$	$u_{i\mathrm{B}}$
N_{D_c}	0.23	0.14
$C_{\mathrm{w,c}}$	0.05	0.25
$k_{\mathrm{rn,BIPM}}$	–	0.10
Q_w	0.10	0.05
k_vol	–	0.03
k_s	–	0.05
depth	–	0.05
$D_{\mathrm{w,BIPM}}$	0.26	0.32

(1) expressed as one standard deviation.

s_i represents the relative uncertainty estimated by statistical methods, type A

u_i represents the relative uncertainty estimated by other methods, type B.

Table 11. Uncertainties associated with the calibration of the chambers at the BIPM

Relative standard uncertainty	$u_{i\mathrm{A}}$	$u_{i\mathrm{B}}$
$D_{\mathrm{w,BIPM}}$	0.26	0.32
$Q_{\mathrm{w,transfer}}$	0.02	0.05
depth	–	0.05
distance	–	0.02
$k_{\mathrm{rn,transfer}}$	–	0.05
$k_{\mathrm{s,transfer}}$	–	0.03
short-term reproducibility	0.07	–
$N_{D_\mathrm{w},\,\mathrm{BIPM}}$	0.27	0.33

For the METAS, the uncertainties are listed in Table 12 and Table 13 for the standard and the chamber calibrations, respectively. The combined standard uncertainty u_c for the comparison results $R_{D_\mathrm{w},\mathrm{METAS}}$ is presented in Table 14.

Table 12. Uncertainties associated with the METAS standard

Relative standard uncertainty [(1)]	$u_{i\mathrm{A}}$	$u_{i\mathrm{B}}$
Reproducibility	0.08	–
Thermistor calibration	–	0.025
Thermistor self-heating	–	0.05
Bridge sensitivity calibration	<0.001	0.005
Absolute temperature from PT100	0.001	0.024
Field perturbation	–	0.025
Water density	–	-[a]
Conductive heat flow	–	0.15
Convection	–	–
Transient thermistor response	–	<0.001
Depth in water	–	0.083
Lateral position	–	0.03
Field size	–	0.03
Heat defect	–	0.30
Specific heat capacity	–	0.05
Beam monitor	<0.01	0.12
$D_{\mathrm{w,\,METAS}}$	0.08	0.38

[a] included in depth in water

Table 13. Uncertainties associated with the calibration of the chambers at the METAS

Relative standard uncertainty	$u_{i\mathrm{A}}$	$u_{i\mathrm{B}}$
$D_{\mathrm{w,\,METAS}}$	0.08	0.38
Current	0.01	0.085
Depth	–	0.12
Lateral position	–	0.03
Field size	–	0.06
$k_{\mathrm{rn,transfer}}$	–	0.08
$k_{\mathrm{s,transfer}}$	–	0.07
Temperature, pressure	–	0.05
Short-term stability	0.02	–
Interpolation beam quality	0.26	–
$N_{D_{\mathrm{w}},\,\mathrm{METAS}}$	0.27	0.43

Table 14. Uncertainties associated with the comparison result

Relative standard uncertainty	u_{iA}	u_{iB}
$N_{D_w,\mathrm{METAS}} / N_{D_w,\mathrm{BIPM}}$	0.38	0.54
Transfer chambers $s_{tr,comp}$	0.03	–
$R_{D_w,\mathrm{METAS}}$	0.66	

6. Degrees of equivalence

Following a decision of the CCRI, the BIPM determination of the dosimetric quantity, here $D_{w,BIPM}$, is taken as the key comparison reference value (KCRV) (Allisy-Roberts *et al* 2009). It follows that for each NMI i having a BIPM comparison result x_i with combined standard uncertainty u_i, the degree of equivalence with respect to the reference value is the relative difference $D_i = (D_{wi} - D_{w,BIPMi})/ D_{w,BIPMi} = x_i - 1$ and its expanded uncertainty $U_i = 2\,u_i$.

The results for D_i and U_i are usually expressed in mGy/Gy. Table 15 gives the values for D_i and U_i for each NMI, i, taken from the BIPM key comparison database (KCDB 2018) and this report. These data are presented graphically in Figure 3.

Table 15. Degrees of equivalence

Beam quality corresponding to measured $TPR_{20,10}$ between 0.63 (excluded) and 0.71 (included)

Lab i	D_i / (mGy/Gy)	U_i
NRC	-2.7	11.0
PTB	1.3	10.4
NIST	3.5	11.4
LNE-LNHB	-4.8	8.8
ARPANSA	-3.5	11.0
NPL	-2.7	12.4
VSL	-4.1	10.8
NMIJ	-3.4	9.4
NIM	-8.3	12.0
METAS	-1.7	13.2

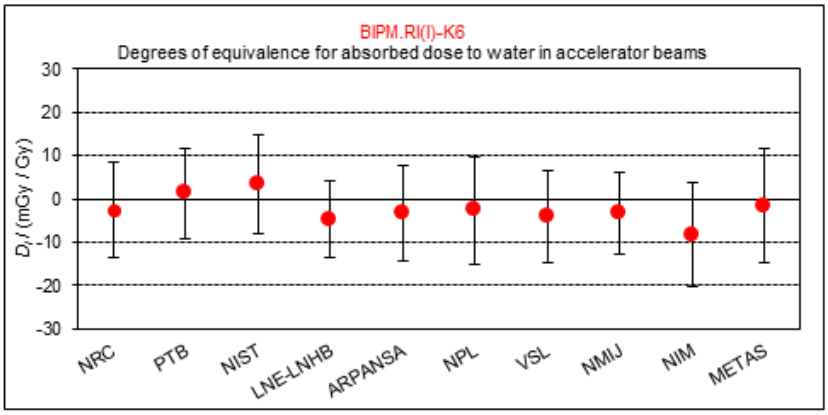

Figure 3. Graph of the degrees of equivalence with the KCRV

Beam quality corresponding to measured $TPR_{20,10}$ between 0.71 (excluded) and 0.77 (included)

Lab *i*	D_i / (mGy/Gy)	U_i / (mGy/Gy)
NRC	0.8	11.0
PTB	3.4	11.4
LNE-LNHB	-5.2	9.4
ARPANSA	-7.6	12.0
NPL	-0.5	13.2
VSL	-4.2	12.8
NMIJ	-4.1	11.0
NIM	-5.9	11.8
METAS	-3.2	13.2

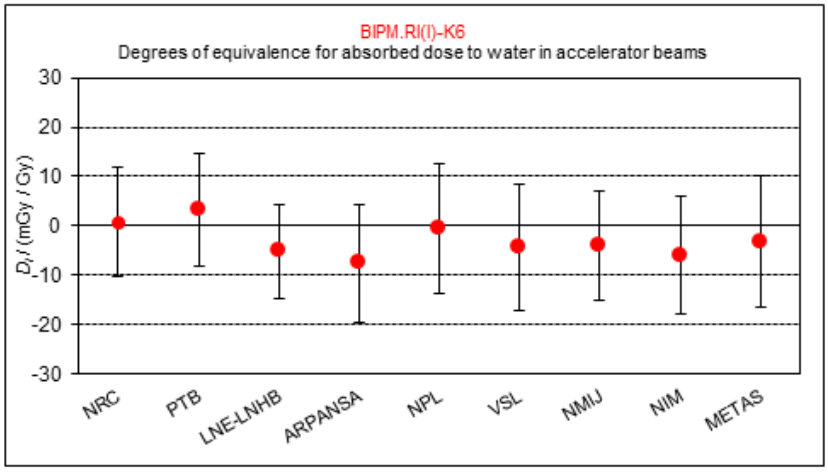

Figure 3. Graph of the degrees of equivalence with the KCRV

Beam quality corresponding to measured $TPR_{20,10}$ between 0.77 (excluded) and 0.81(included)

Lab *i*	D_i / (mGy/Gy)	U_i / (mGy/Gy)
NRC	-5.8	11.0
PTB	1.8	12.8
NIST	-4.2	11.8
LNE-LNHB	-6.2	10.0
ARPANSA	-6.8	11.8
NPL	-4.3	16.2
VSL	-0.9	15.0
METAS	-1.2	13.2

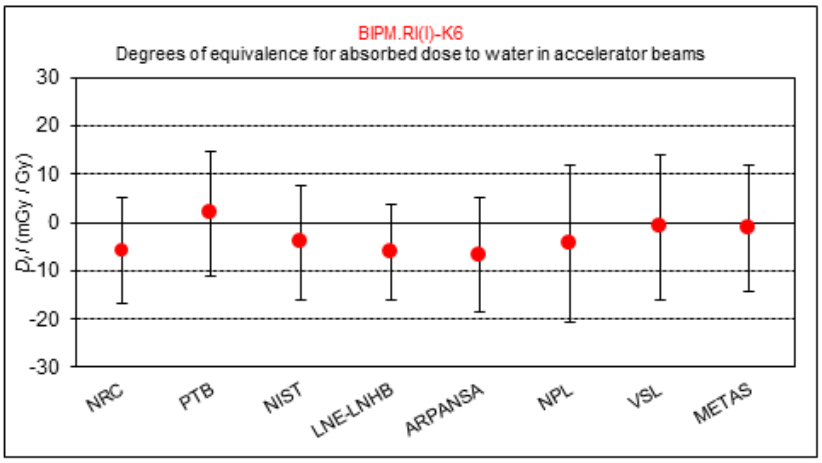

Figure 3. Graph of the degrees of equivalence with the KCRV

7. Conclusions

A key comparison has been carried out between the METAS and the BIPM standards for absorbed dose to water in accelerator photon beams, using two ionization chambers as transfer instruments. The comparison result is evaluated as the ratio of the calibration coefficients measured by the METAS and the BIPM. The results show the standards to be in agreement within the standard uncertainty of the comparison of 6.6 parts in 10^3.

When compared with the results for the other laboratories that have carried out comparisons in terms of absorbed dose to water, the METAS standard for absorbed dose to water is in good agreement with the ensemble of results.

Note that the data presented in the tables, while correct at the time of publication of the present report, become out of date as laboratories make new comparisons with the BIPM. The formal results under the CIPM MRA are those available in the BIPM key comparison database (KCDB 2018).

References

Allisy P J, Burns D T and Andreo P 2009 International framework of traceability for radiation dosimetry quantities *Metrologia* **46(2)** S1-S8

Boutillon M 1998 Volume recombination parameter in ionization chambers *Phys. Med. Biol.* **43** 2061-2072

Burns D T 2018 The dose conversion procedure for the BIPM graphite calorimeter standard for absorbed dose to water, in preparation

International Atomic Energy Agency 2000 Absorbed Dose Determination in External Beam Radiotherapy. An International Code of Practice for Dosimetry Based in Standards of Absorbed Dose to Water *Technical Report Series* No 398 (IAEA Vienna)

KCDB 2018 BIPM Key Comparison Database ^{60}Co absorbed dose to water comparisons BIPM.RI(I)-K6

Klassen N V and Ross C K 1991 Absorbed dose calorimetry using various aqueous solutions *Radiat. Phys. Chem.* **38** 95-104

Klassen N V and Ross C K 1997 Water calorimetry: The heat defect *J. Res. Natl. Inst. Stand. Technol.* **102** 63-74

Medin J, Seuntjens J, Klassen N, Ross C K and Stucki G 1999 The OFMET sealed water calorimeter *Proceedings of NPL Workshop on Recent advances in Calorimetric Absorbed Dose Standards* NPL Report CIRM 42

Picard S, Burns D T and Roger P 2009 Construction of an Absorbed-Dose Graphite Calorimeter *Rapport* BIPM-2009/01 (Sèvres: Bureau International des Poids et Mesures)

Picard S, Kessler C, Roger P and Burns D T 2016 Key comparison BIPM.RI(I)-K6 for the standards of absorbed dose to water at 10 g cm^{-2} of the NIM, China and the BIPM in accelerator photon beams *Metrologia* **54** *Tech. Suppl.* 06009